2011

Exploring the Functional Interaction Between CaMK-II and p53

Raymond Lai
Virginia Commonwealth University

EXPLORING THE FUNCTIONAL INTERACTION BETWEEN CAMK-II AND P53

A Thesis submitted in partial fulfillment of the requirements for the degree of Master of Science, Biology at Virginia Commonwealth University.

by

RAYMOND EUGENE LAI

B.S., College of William and Mary 2009

Director: ROBERT M. TOMBES, Ph. D

PROFESSOR, DEPARTMENT OF BIOLOGY

Virginia Commonwealth University

Richmond, VA

May, 2011

Acknowledgement

The work involved with the production of my thesis in the past two years would not have been possible without all the support, guidance, and encouragement I was fortunate enough to receive from a number of wonderful people. First and foremost I would like to thank my advisor Dr. Robert Tombes for all the patience and understanding he has consistently shown toward me throughout the process of my research. During the entire span of time I have been able to spend in his lab, the breadth of knowledge and passion he has for his work has always been an inspiration toward me. My thanks also go out to my committee members, Dr. Sumitra Deb, Dr. Amanda Dickinson, and Dr. Fernando Tenjo, for their generosity in offering their time and effort in helping me complete my project. My immense appreciation also goes out to Catherine Vaughn of Dr. Sumitra Deb's lab at the VCU Massey Cancer Center for her arduous efforts in making the stable knockdown cell line that played an integral role in my research. I would also like to graciously thank all my colleagues in the lab, Ali Myers, Sarah Rothschild, Jamie McLeod, Ludmila Francescatto, Bennett Childs, Amritha Yellamilli, and Rachel Troch, all whom have been essential in helping me with all my work. Much of my gratitude also goes out to my friends and family who have continuously offered me tremendous support, faith, and love throughout the course of everything that I have been able to accomplish.

Table of Contents

List of Figures

Page

List of Abbreviations

α	Alpha
A	Alanine
Ala	Alanine
A568	Alexa Fluor 568
Asp	Aspartic Acid
ATM	Ataxia Telangiectasia Mutated
ATP	Adenosine Triphosphate
β	Beta
Bcl-2	B-Cell Lymphoma 2
BCIP	5-bromo-4-chloro-3-indolyl phosphate
BS	pBluescript-KS^+
BSA	Bovine Serum Albumin
C-terminus	Carboxy Terminus
Ca^{2+}	Calcium Ion
CaM	Calmodulin
CaMK-II	Calcium (Ca)/calmodulin-dependent kinase 2
Cdk2	Cyclin-Dependent Kinase 2
δ	Delta
D	Aspartic Acid
DAPI	4'6- diamidino-2-phenylindole
DMEM	Dulbecco's Modified Eagle's Medium
DNA	Deoxyribonucleic Acid
EDTA	Ethylenediamine Tetra-acetic Acid
EGTA	[ethylenebis(oxyethylenenitrilo)] tetra-acetic acid
ER	Endoplasmic Reticulum
FAK	Focal Adhesion Kinase
FBS	Fetal Bovine Serum
FLAG	DYKDDDDK Epitope Tag
Fli-I	Flightless-I
γ	Gamma
G	Glycine
g	Gram
G_0	Gap 0 Phase
G_1	Gap 1 Phase
GFP	Green Fluorescent Protein
Gly	Glycine
GSK-3	Glycogen Synthase Kinase 3
HB	Homogenization Buffer

HBSS	Hank's Buffered Salt Solution
HEK	Human Embryonic Kidneys Cells
HEPES	(2-Hydroxyethyl) piperazine-1-ethanesulfonic acid
JNK	Jun N-terminal Kinase
kDa	Kilodalton
K	Lysine
KV	Kupffer's Vesicle
Lys	Lysine
L2K	Lipofectamine 2000
µ	Micro
m	Milli
M	Molar
mdm2	Murine Double Minute 2
mPCTs	Mouse Proximal Convoluted Tubule Cells
$MgCl_2$	Magnesium Chloride
NaCl	Sodium Chloride
NBT	Nitro Blue Tetrazolium
NIH/3T3	Mouse Embryonic Fibroblast Cells
N- terminus	Amino Terminus
p21	Cyclin-Dependent Kinase Inhibitor 1
p38	P38 Mitogen-Activated Protein Kinase
p53	Tumor Suppressor Protein 53
PAGE	Polyacrylamide Gel Electrophoresis
PBS	Phosphate Buffered Saline
PCR	Polymerase Chain Reaction
PKD-2	Polycystic Kidney Disease 2
RISC	RNA Induced Silencing Complex
Ryr3	Ryanodine Receptor 3
SBTI	Soy Bean Trypsin Inhibitor
SDS	Sodium Dodecyl Sulfate
Ser	Serine
shRNA	Short Hairpin Ribonucleic Acid
siRNA	Small Interfering Ribonucleic Acid
T	Threonine
TBSTA	Tris-buffered saline with 0.05% Tween 20 and 0.05 % sodium azide
Tbx-5	T-box Transcription Factor 5
TRIS	2-Amino-2-(hydroxymethyl)-1,3-propanediol

ABSTRACT

Exploring the Functional Interaction between CaMK-II and p53

By Raymond E. Lai, B.S.

A Thesis submitted in partial fulfillment of the requirements for the degree of Master of Science, Biology at Virginia Commonwealth University.

Virginia Commonwealth University, 2011

Major Director: Robert M. Tombes, Ph. D

Professor, Department of Biology

Calcium (Ca^{2+})/calmodulin-dependent kinase 2 (CaMK-II) is a multifunctional member of a family of Ca^{2+}/calmodulin-dependent serine/threonine protein kinases that respond to transient intracellular calcium signaling. CaMK-II has been reported to be involved with transcription regulation, cell motility, neuronal development, cell cycle regulation, and more recently early development of vertebrates (Easley et al., 2008; Rothschild et al., 2009; Francescatto et al., 2010). Through previous work in the lab using tandem mass spectrometry and "substrate-trapping mutants", tumor suppressor protein 53 (p53) was identified as a novel CaMK-II binding partner in tissue culture. In this study, I sought to provide characterization of the functional interaction of p53 and CaMK-II. First, a stable p53 knockdown human cell line (HEK) was established through lentiviral transduction of p53 shRNA and verified with immunoblots and immunostaining assays. Next, the localization of CaMK-II and the cell growth rate in these cells was determined. In wild type HEK cells, catalytically inactive CaMK-II inhibited cell growth, which is consistent with previous studies in mouse fibroblasts with

pharmacological inhibition. p53-deficient cells were less sensitive to CaMK-II deficiencies using dominant negative CAMK-II, but not pharmacological disruption. The overall results of this study have provided significant clues to the mechanism between CaMK-II and p53 in the control of cell cycle progression.

INTRODUCTION

Calcium (Ca^{2+})/calmodulin-dependent kinase 2 (CaMK-II) is a multifunctional member of a family of Ca^{2+}/calmodulin-dependent serine/threonine protein kinases that respond to transient intracellular calcium signaling (Hudmon et al., 2002). CaMK-II is a ubiquitously expressed dodecameric enzyme that is encoded by four different genes (α, β, γ, and δ) that form over 40 splice variants (Tombes et al., 2003). Each subunit is made up of three different domains: the catalytic, variable, and association domains. The amino-terminal catalytic domain encodes the calmodulin and autoinhibitory binding regions and is integral for ATP and substrate binding. With its susceptibility to alternative splicing, the variable domain is responsible for the diversity of the kinase. The oligomerization of its monomers to form a dodecomeric protein takes place on the carboxy-terminal association domain. CaMK-II oligomerization enables it to be autophosphorylated independently of Ca^{2+} when Ca^{2+} levels subside within the cell (Kolb et al., 1998; Lantsman and Tombes, 2005).

Roles of CaMK-II. Inherent of its own transcriptional and post-transcriptional variability, CaMK-II binds to and phosphorylates a number of different target substrates. Because of this, it is an enzyme with a wide array of functions (Yoshimura et al., 2002). As indicated in previous literature, CaMK-II has been implicated in a variety of roles including cell cycle progression, regulation of β-catenin dependent transcription, and promoting cell motility (Easley et al., 2008; Seward et al., 2008). From some recently published work, CaMK-II has been shown to be essential for the early development of vertebrates. A specific member of the CaMK-II family (β2

CAMK-II) is induced by T-box transcription factor (Tbx-5). Tbx-5 is a protein known to be expressed during atrium and ventricle development in the heart of zebrafish and when mutated in humans result in limb and heart abnormalities typically described by the autosomal dominant disorder known as Holt-Oram syndrome (Basson et al., 1997; Rothschild et al., 2009). The expression of β2 CAMK-II is also in the developing fins and the looping of the heart, but is diminished in *tbx-5* morphants. In both zebrafish embryos and mouse fibroblast cells, CaMK-II expression is significantly increased upon the introduction of excess Tbx-5. CaMK-II is thus dependent on Tbx-5 and is necessary for heart and fin development (Rothschild et al., 2009). Additional work on zebrafish has also shown that activated CaMK-II is identified as a target of Ca^{2+} elevations that occur on the left side of the Kupffer's vesicle (KV) during development. The transient activation of CaMK-II linking KV function with lateral plate mesoderm signaling has been shown to be responsible for left-right asymmetry in zebrafish. Fluid flowing counterclockwise over adjacent ciliated cells or morphogen binding induces Ca^{2+} elevations on the left side of the KV. Membrane targeted hetero-oligomers of αKAP and γ1 CaMK-II are activated through further Ca^{2+} elevations by PKD2 dependent calcium release via cilia, ER and the ryanodine receptor, Ryr3. Ca^{2+} elevation into the adjacent cells in the KV via connexin gap junctions and the subsequent clustering of activated CaMK-II induces left-right asymmetry through southpaw processing or secretion (Francescatto, 2010).

CaMK-II, known to co-localize with the actin cytoskeleton, has also been implicated to induce cell motility through focal adhesion turnover. Paxillin and focal adhesion kinase (FAK), two proteins known to be critical in structure in focal adhesion complexes, are actively dephosphorylated by the catalytic activity of CaMK-II promoting focal adhesion disassembly and thus increases cell motility (Easley et al., 2008).

The role of CaMK-II during cell cycle progression and β catenin dependent gene regulation has also been studied. Active CaMK-II binds with the gelsolin-related actin binding and capping protein, Flightless-I (Fli-I), and sequesters it in the cytosol. When CaMK-II is inhibited, Fli-I detaches and translocates into the nucleus thereby disrupting DNA synthesis by lowering the levels of β catenin dependent genes including cyclin D1. When cyclin D1 levels drop, the cell arrests in G_1 and thus cannot proceed toward the S phase of the cell cycle (Seward et al., 2008; Resnitzky et al.,1994). Another recently published study has shown that inhibited CaMK-II causes G_1 cell cycle arrest by reducing cyclin D1 levels and enhancing the association with $p27^{Kip1}$ with Cdk2 (Morris et al., 1998).

Substrate-Trapping Mutants. Historically studying protein-protein interactions within a signaling cascade has been difficult due to the high complexity of the phosphorylation and dephosphorylation activities performed by kinases and phosphatases, respectively. "Substrate trapping" phosphatases that lack their catalytic activity but maintain their substrate binding ability were developed in the past and used to study protein interactions. Following the co-precipitation of phosphatase substrates with the inactive phosphatase, the identification of both proteins by mass spectrometry was possible (Blanchetot et al., 2005).

In previous work done by Ali Myers of the Tombes Lab, substrates of CaMK-II were identified and isolated using catalytically inactive CaMK-II as "bait". Several mutant CaMK-II with different functions were created which include $K^{43}A$, $K^{43}G$, $D^{137}A$, $D^{189}A$, and $T^{287}D$. Phospho-transfer is an activity that lysine (K) located on the 43^{rd} position of the CaMK-II catalytic domain participates in (Hanks et al., 1988). When this residue is altered, it can have a

profound effect on its ability to phoshorylate its substrates. Some of the mutants that have been constructed have this specific residue changed from one that was large and negatively charged to one that is smaller and neutral like alanine or glycine. The resulting $K^{43}A$ and $K^{43}G$ CaMK-II mutants retain their high affinity for their substrates, but have lost their ability to complete the catalytic cycle, which therefore causes substrate trapping at their active sites (Figure 1). The catalytically inactive $K^{43}A$ and $K^{43}G$ CaMK-II constructs in conjunction with tandem mass spectrometry were utilized in order to isolate and identify p53 as a novel CaMK-II binding partner. For this study, the use of these "substrate-trapping" mutants was essential in determining the functional role of CaMK-II with p53 in tissue culture.

Roles of p53. Tumor suppressor protein p53 is often described as the "guardian of the genome" referring to its significant contribution in preventing genomic mutation by conserving stability (Lane, 1992). The p53 protein is involved in several anti-cancer mechanisms which include roles in apoptosis, genetic stability, growth arrest, and even the inhibition of angiogenesis (Muller et al., 2011). It should be noted that the majority of cancer related illness is attributed to some form of p53 mutation, gene deletion, or abrogated cellular component in the p53 pathway (Amaral et al., 2010). p53 stabilization like most other proteins happen upon a phosphorylation event by a kinase such as JNK, p38, and ATM. The stabilization of p53 is regulated by the E3 ubiquitin ligase, mdm2, which acts by inactivating the tumor suppressor through nucleus exportation and its subsequent degradation by the 26S proteosome (Brooks et al., 2007). When p53's lysine residues are acetylated, ubiquitination events of p53 are reduced (Li et al., 2002). Activated p53 is most known for suppressing tumor formation by binding to DNA

which activates the expression of genes like WAF1/CIP1 that encode for the protein p21. When p21 binds to and forms a complex with Cdk-2, the cell cycle arrests between the G_1 and S phases (Abbas et al., 2009). p53 is also known to induce apoptosis through its mitochondrial pathway. In response to a stress signal, p53 is targeted to the mitochondria and interacts with anti- and pro-apopotic Bcl-2-family members either inhibiting or activating them. This at first leads to robust mitochondrial outer membrane permeabilization then is followed by the initiation of caspase activity. Apoptosis can also be generated via the death receptor pathway which occurs by the recruitment of adapter proteins by receptors in the cellular membrane which also trigger the activation of caspases (Amaral et al., 2010).

siRNA and shRNA Lentiviral Transduction. The latest advances in sequence-based approaches to "knockdown" gene function have given rise to a wide array of cost-effective reverse genetic approaches for studying gene function. This study utilized the approach involving lentiviral mediated transduction to stably knockdown the p53 gene by delivering shRNA into cells. shRNA which goes through the RNAi mechanism in cells has been proven to be applicable to a number of organisms and has been used to generate a wide array of loss-of-function phenotypes (Kuttenkeuler and Boutros, 2004). Lentiviruses can deliver a significant amount of genetic information into the DNA of the host cell and have the unique ability among retroviruses of being able to replicate in non-dividing cells. Unlike other retroviruses which can only affect dividing cells, the pre-integration complex of lentiviruses can penetrate the intact membrane of the nucleus of the target cell. Lentiviral transduction integrates the shRNA into the chromosome of the target cell. The resulting shRNA produced by the transcriptional machinery

of the cell will then translocate to the cytoplasm where it binds to and gets cleaved by the Dicer endonuclease into single stranded small interfering RNA (siRNA). The RNA induced silencing complex (RISC) then cleaves the target mRNA that is complementary with the siRNA (Pattanayak et al. 2005). This technology was used to create a stable p53 knockdown human embryonic kidney (HEK) tissue culture cell line. The utilization of this newly established HEK cell line was a key component in my investigation of characterizing the functional interaction between CaMK-II and p53.

MATERIALS AND METHODS

mPCT and HEK Cell Culture. Dulbecco Modified Eagle's Medium (DMEM) with 10% FBS, L-Glutamine, Pennicilin Streptomycin was used to maintain mouse proximal convoluted tubule (mPCT) and human embryonic kidney (HEK) cell lines incubated at 37°C with 5% CO_2 in 100mm dishes. 3µg/mL of filtered puromycin (InVivoGen, San Diego, CA) diluted in 1x HBSS was included in the medium for maintaining the p53 RNA and GFP RNA infected HEK cell line. Cells were sub-cultured every 3-4 days to maintain sub-confluence.

Vectors. Lys-43-Ala ($K^{43}A$) and Lys-43-Gly ($K^{43}G$) were introduced via PCR mediated site-specific mutagenesis into the coding sequence for FLAG-GFPδ_e CaMK-II. The mutant constructs were directionally inserted into the pCDNA3 vector for transfections. Vectors were confirmed through restriction enzyme digestion, DNA sequencing and protein expression was determined through immunoblotting.

Transfection into Cell Lines. Transfection of the mutants with a total of 3µg plasmid DNA using Lipofectamine 2000 (Invitrogen, Carlsbad, CA) diluted in Opti-MEM (Invitrogen) were performed on human embryonic kidney cells (HEK) and mouse proximal convoluted tubules (mPCTs) cell lines at 50-70% confluency in 6 well plates (Corning Inc, Corning, NY). pBlueScript-KS^+ (BS) was co-transfected if necessary as a carrier vector. p53 siRNA and p53 scrambled siRNA (Sigma-Aldrich, St. Louis, MO) was double transfected into HEK cell lines 24

hours apart before being transfected by CaMK-II constructs. Cells were re-fed with culture medium (DMEM, as described in cell culture section) just prior to the addition of transfection agents.

siRNA. siRNA provided by Dr. Sumitra Deb of the VCU Medical Center (up to 40 pmol) were transfected with a total of 3.0 µg of pBluescript KS^+ or other DNA vector into HEK cells using Lipofectamine 2000 as described under transfections. The p53 siRNA and p53 scrambled siRNA (Sigma-Aldrich) are listed from 5' to 3'.

p53 siRNA: GCA UGA ACC GGA GGC CCA U

p53 scrambled siRNA: CAU GUC AUG UGU CAC AUC UC

Lentiviral Generation and Transduction. 5µg of shRNA (either p53 or GFP control) constructs with 2.5µg of a packaging vector and 2.5µg of an envelope vector (Sigma-Aldrich) were co-transfected into HEK cells as described in the transfection section. After 48 hours of incubation at 37°C with 5% CO_2, the medium containing the recombinant lentiviral particles from the transfected cells was collected. HEK cells in a 100mm plate were washed with 1x PBS then treated with 1 mL of the lentiviral medium. The cells were incubated at 37°C with 5% CO_2 with gentle rocking every 15 minutes for 2 hours. 10 mL of complete media was added and incubated for 48 hours before they were selected with 4µg/mL of puromycin antibiotic. All the work involving the lentiviral generation and transduction was kindly performed by Catherine Vaughn of Dr. Sumitra Deb's lab of the VCU Massey Cancer Center in Richmond, Virginia.

Immunostaining. Cells were prepared for immunostaining by being sub-cultured on poly-D-lysine (Fisher Scientific, Pittsburgh, PA) pre-treated 12 mm cover slips (Fisher Scientific) in 6 well plates (Corning Inc). Cells which were approximately 70% confluent were washed with 1x PBS, fixed with 4% Paraformaldehyde in 1x PBS for 10 minutes, and washed with 0.01% NP40 in 1x PBS. The cells were then fixed again with 4% Paraformaldehyde in 1x PBS for 5 minutes, washed with 1x PBS then blocked with 5% BSA in 1x TBSTA for 1 hour at room temperature. The appropriate primary antibody was diluted to 10µg/mL with 2% BSA in 1x TBSTA and incubated with the cells at 37°C for 1 hour. Cells were washed three times for 5 minutes with 1x PBS. The appropriate secondary antibody was diluted to 10µg/mL in 2x BSA in 1x TBSTA and applied to the cells for 30 minutes at 37°C. Cells were washed three times for 5 minutes with 1x PBS and placed on slides with mounting medium for imaging (KPL, Gaithersburg, MD).

DAPI Staining. 4',6-diamidino-2-phenylindole (DAPI) is a fluorescent stain that binds strongly to nuclear DNA. A solution containing 4% Paraformaldehyde in 1x PBS, 0.05% NP40, and 5µg/mL DAPI was made and applied to the cells and incubated at 4°C for 30 minutes. Cells were then washed and stored in 1x PBS for imaging.

Mitochondrial Staining. 1mM of MitoTracker (Invitrogen) stock solution was diluted to 100nM in culture medium (DMEM, as described in the cell culture section). Once cells reached

70% confluency, media was removed and pre-warmed staining solution containing the MitoTracker probe was added and put in a 5% CO_2 incubator for 30 minutes set to 37°C. Mitochondrial staining of the cells were then verified using a fluorescent microscope then fixed using 4% Paraformaldehyde in 1x PBS for 10 minutes.

Cell Harvest. mPCTs were harvested as follows: 0.25% Trypsin-EDTA added and resuspended in culture medium (DMEM, as described in the cell culture section). The cells were then washed with 1x Phosphate Buffered Saline (PBS, Gibco/Invitrogen,), centrifuged at 1000 x g for 5 min at 4°C, and resuspended in homogenization buffer containing 20mM HEPES (pH7.4), 2.6mM EGTA, 20mM $MgCl_2$ and 80mM β-glycerol phosphate with 1µg/µL okadaic acid, and 1µg/ml protease inhibitors (chymostatin, leupeptin, aprotinin, pepstatin, and soybean trypsin inhibitor (SBTI)). Cells were sonicated twice with 3 second bursts on ice then centrifuged at 12,000 x g for 5 minutes. HEK cells were harvested the same way but without the addition of 0.25% trypsin-EDTA.

Western Transfer and Immunoblotting. Cell lysates were subject to Sodium Dodecyl Sulfate- Polyacrylamide Gel Electorphoresis (SDS-PAGE) using the Bio-Rad Mini-Protean System. Western protein transfer was separated using 4-15% polyacrylamide gels at 150V and then transferred on to 0.45µm pore size nitrocellulose medium (Bio-Rad, Hercules, CA) for 1 hour at 110V. Proteins on nitrocellulose were blocked with 5% BSA in 1x TBSTA (0.05% Tween 20, 0.05% Sodium Azide) for 30 min. The appropriate primary antibody was diluted to 1µg/mL in 5% BSA then added to the nitrocellulose paper for about 18 hours rocking overnight

at room temperature. Three 5 minute washes were performed with 1x TBSTA then 2μg/ml of alkaline phosphatase conjugated secondary antibody was added and shaken for 2 hours. Blots were then washed three times for 5 minutes with 1x TBSTA before being developed in 0.1 M Tris, 0.1 M NaCl, 5mM $MgCl_2$ phosphatase buffer (pH 9.4) containing 0.25 mg/ml 5-bromo-4-chloro-3-indolyl phosphate (BCIP, Sigma-Aldrich) and 0.25 mg/ml nitro blue tetrazolium (NBT, Sigma-Aldrich) in the dark. Selected blots were digitally scanned.

Antibodies. The mouse anti-p53 monoclonal antibody (1C12) was purchased from Cell Signaling Technology, Danvers, MA. Goat anti-mouse and Rabbit anti-mouse secondary antibodies were purchased from Invitrogen.

Drug treatment. KN-93, a membrane permeant calmodulin antagonist CaMK-II inhibitor (Fisher Scientific) was directly added to cells in culture at various concentrations diluted in culture medium.

Imaging. A 12-bit camera and an Olympus IX-70 inverted microscope was used in order to capture phase contrast and fluorescent images (Olympus, Melville, NY). Fluorescent images were taken with two second exposures using a 595 nm dichroic long pass filter (Chroma, Rockingham, VT) illuminated by a mercury arc lamp. The images were processed using Olympus Microsuite, v.5.

RESULTS

Knockdown and verification of p53 stable cell lines. To begin the investigation of the functional interaction of CaMK-II and p53, a stable p53 knockdown cell line was established. The HEK cell line was chosen since they have good transfection efficiency (60-70%). The stable HEK cell line was made using lentiviral transduction of shRNA to knockdown p53. An additional lentiviral transduction was performed with GFP shRNA to establish a virally infected control HEK cell line. Each shRNA vector contained a gene resistant to the antibiotic puromycin for selection. Following the generation of the viral particles and the subsequent transduction (as described in the methods section), multiple clones were selected using puromycin antibiotic and then grown to full confluence. Immunoblots and an immunostaining assay verifying p53 knockdown using mouse monoclonal antibodies specific to p53 were performed on the lysates obtained from the harvest of each shRNA infected HEK cell line (Figure 2A and B). These tests confirmed the successful knockdown of p53 in the HEK cell line and thus could be used for further analysis.

$K^{43}G$ CaMK-II inhibits cell growth in the presence of p53. Cell cycle arrest has been reported to be linked to CaMK-II inhibition through both the transition from G_1 to S and G_2 to M phases (Tombes et al., 1995; Morris et al., 1998). In order to observe the effect of CaMK-II on cell cycle regulation in p53 deficient cells, HEK cells were DAPI stained 48 after WT or $K^{43}G$ CaMK-II construct transfection. The cells counted in ten random fields for each condition were

summed then averaged amongst three different experiments. The percent total cell difference between WT and $K^{43}G$ transfection was calculated and compared between the p53 knockdown and GFP control HEK cell lines. Across all experiments, cells transfected with $K^{43}G$ CaMK-II had a lower total cell count compared to those transfected with WT CaMK-II. This result suggests that the over expression of dominant negative CaMK-II causes the inhibition of cell growth which is consistent with previous work done by pharmacologically inhibiting CaMK-II in mouse fibroblasts (Tombes et al., 1995). The percent difference in total cells between WT and $K^{43}G$ transfected HEK cells with p53 knocked down was more than two times reduced when compared to the control cells. This result suggests that cell growth inhibition only occurs in HEK cells that have p53 (Figure 3).

HEK cell growth is repressed by KN-93 induced CaMK-II inhibition, but is not more sensitive in the absence of p53. KN-93, a membrane permeant synthetic inhibitor of CaMK-II that inactivates CaMK-II activity by antagonizing calmodulin binding, was used in a previous study to conclude that CaMK-II is required for cell cycle progression through the G_1 phase in NIH/3T3 cells (Tombes et al., 1995). CaMK-II inhibition is also involved in the up-regulation of the cell cycle inhibitor p21 and down-regulation of the positive regulators cyclin D1, cyclin E, and Cdk2 in human ovarian cell lines (Ma et al., 2009). Additionally, upon CaMK-II inhibition p53 pathway components such as p21and mdm2 are induced and degraded, respectively, as seen in vascular smooth muscle proliferation studies (Li et al., 2011). In order to further examine whether CaMK-II inhibition reduces cell growth, KN-93 was used to treat the stable p53 knockdown HEK cell line in a dose dependent manner in two different experiments (Figure 4A

and B). In the initial experiment, HEK cells were treated with KN-93 then DAPI stained after 48 hours. The total cells counted in fifteen random fields in each condition were summed then averaged amongst three different experiments. The percent total cell difference between the KN-93 treated and untreated HEK cells was calculated and compared between the p53 knockdown and GFP control HEK cell lines. Compared to controls, KN-93 treated HEK cells consistently had lower total cell number after 48 hours; however, there was no evidence of a significant difference between the p53 knockdown and control cells (Figure 4A).

An additional experiment was done to confirm this result. Direct cell counts were done in the presence of KN-93 before treatment then again after 24 hours for each condition. The total cells in ten random fields in each condition were summed then averaged amongst two experiments. The percentage of total cell increase from when the cells were initially plated to 24 hours after drug treatment was calculated and compared between the p53 knockdown and GFP control HEK cell lines. In the presence of KN-93, HEK cell growth inhibition occurred in a dose-dependent manner, but again did not show that the p53 deficient cells were more sensitive (Figure 4B).

Less CaMK-II aggregates form in absence of p53. Full length CaMK-II is known to localize to the cytosol which was confirmed using fluorescent microscopy (Caran et al., 2001). An observation that is consistent across all transfections was the apparent increase of the GFP expression of CaMK-II in small aggregates (approximately 1-2 μm in size) in cells transfected with dominant negative forms of CaMK-II, $K^{43}A$ and $K^{43}G$, in both HEK and mPCT cells (Figure 5). FLAG-GFP δ_e CaMK-II $K^{43}A$ transfected cells overall displayed less aggregates in

comparison to FLAG-GFP δ_e CaMK-II $K^{43}G$. The aggregate analysis was first analyzed using siRNA to knockdown p53 in HEK cells. It was necessary to optimize the siRNA transfection in order to effectively knockdown p53. The siRNA transfection protocol was conducted by doing a double transfection (first transfection = 30 pmol; second transfection = 10 pmol) of p53 siRNA or the control p53 scrambled siRNA into HEK cells. WT or $K^{43}G$ CaMK-II was co-transfected with the second siRNA transfection. There was a noticeable decrease of CaMK-II aggregates in cells with p53 knocked down in both WT and $K^{43}G$ transfected HEK cells at 48 hours post transfection (Figure 6A). Amongst the $K^{43}G$ transfected cells, the total number of aggregates in the cells with p53 knocked down were reduced by half compared to the p53 scrambled siRNA control. Follow up experiments were performed by transfecting the CaMK-II constructs into stable p53 knockdown HEK cells. At 48 hours post transfection, the results were consistent with the siRNA transfection results. There was a significant difference in the amount of $K^{43}G$ and WT CaMK-II aggregates between the p53 knockdown and GFP control HEK cells. The number of aggregates was summed from at least ten different fields per condition then averaged between three experiments (Figure 6B).

$K^{43}G$ CaMK-II aggregates might not be associated with the mitochondrial p53 pathway.

The p53 mitochondrial pathway has been described to involve p53 translocating to the mitochondria in the cytosol and interacting with a number of anti and pro-apoptotic Bcl-2-family members to either initiate or inhibit them. These interactions lead to eventual mitochondrial outer membrane permeabilization and the eventual increase of caspase activity which initiate chromatin degradation (Vaseava and Moll, 2008). The initial thought of CaMK-II aggregates

occurring within the cytosol of the cells prompted us to think about the possibility that CaMK-II might be co-localizing with intracellular mitochondria and thus be involved with the p53 mitochondrial pathway. To test this, the mitochondrion selective probe MitoTracker from Invitrogen was used to stain all intracellular mitochondria in live CaMK-II transfected HEK cells which worked by passively diffusing across the plasma membrane and accumulating in active mitochondria. Following analysis via fluorescent microscopy, CaMK-II aggregate co-localization with mitochondria was not clearly evident (Figure 7). Furthermore, there was also no clear evidence of DNA fragmentation in dominant negative CaMK-II transfected HEK cells which normally occurs upon the initiation of apoptosis (Figure 8). These results do not support the possible association of CaMK-II with the mitochondrial p53 dependent mechanism. The effects of the functional interaction between CaMK-II and p53 therefore suggest a role in cell cycle control.

DISCUSSION

The rapid and efficient detection of substrates and binding partners of substrate trapping FLAG-GFP δ_e CaMK-II mutants that were used in a previous investigation done by Ali Myers of the Tombes Lab involving tandem mass spectrometry were utilized in this study in an attempt to provide evidence of a direct link between the functional interaction of CaMK-II and its recently discovered binding partner p53. Despite the lack of evidence showing that p53 is phosphorylated by CaMK-II, the binding interaction of p53 to catalytically inactive CaMK-II was previously shown. The interaction in this study was characterized using siRNA and lentiviral shRNA technology to knockdown p53 transiently and stably, respectively. Tumor suppressor protein p53, known to be mutated in most cases of cancer, has been widely studied in order to elucidate its roles in apoptosis, genetic stability, and cell cycle regulation (Amaral et al, 2010). CaMK-II has also been implicated in cell cycle control and apoptosis in several studies (Li et al., 2009; Wang et al., 2008; Tombes et al., 1995). The novel binding interaction between the two proteins therefore does not seem to be coincidental considering the similarities in their roles within the cell.

The results obtained in this investigation, provide clues to suggest a model by which catalytically inactive CaMK-II sequesters p53 in the cytosol to regulate cell cycle progression (Figure 9). Initially, p53 cytosolic localization was expected to cytoprotect or promote cell survival similarly to its nuclear exportation mechanism regulated by the stabilization of its inhibitor E3 ubiquitin ligase mdm2 (Lohrum et al., 2001). However, from the results obtained in my study, the sequestering of p53 by catalytically inactive CaMK-II in the cytosol seems to

promote cell cycle arrest and not apoptotic activity. Mitochondria staining did not show clear co-localization with CaMK-II aggregates (Figure 7) and DAPI staining did not show any evidence of nuclear fragmentation (Figure 8).

Previous studies involving GSK-3 could explain how CaMK-II and p53 work in conjunction to regulate cell cycle progression. GSK-3α and GSK-3β are deactivated from the phosphorylation of its amino terminal residues Ser^{21} and Ser^{9}, respectively (Cohen et al., 2001). GSK-3β Ser^{9} and GSK-3α Ser^{21} are consensus CaMK-II phosphorylation sites and thus activated CaMK-II can inactivate GSK-3 through phosphorylation (Song et al., 2010). When CaMK-II is inactive, phosphorylation of GSK-3β does not occur and therefore remains activated. Activated GSK-3 enters the nucleus and down regulates SKP2, a protein that normally inhibits $p27^{Kip1}$ expression. Stabilized $p27^{Kip1}$ then binds to cyclin dependent kinase 2 (Cdk2) causing cell-cycle arrest at the G_0/G_1 phase (Wang et al., 2008). A study done using NIH/3T3 cells showed that Cdk2 kinase phosphorylates p53 at Ser^{315} (Price et al., 1995). It has also been shown that phosphorylation of proteins by Cdk2 initiates their export from the nucleus (Fradet-Turcotte et al., 2010). Upon activation it is possible that Cdk2 initiates the nuclear export of p53 by phosphorylating the tumor suppressor at Ser^{315}. However, since Cdk2 is bound to $p27^{Kip1}$ in my proposed model, this may not occur. The mechanism by which explains how p53 is exported from the nucleus thereby remains to be determined.

The results of my study obtained from transfecting cells with catalytically inactive $K^{43}G$ CaMK-II seem to support this potential model, however, the importance of the CaMK-II aggregates that inevitably form remains to be determined. It can be speculated from the data I obtained that once p53 has translocated in the cytosol, catalytically inactive CaMK-II come

together to form aggregates localizing in the areas where most of the p53 is found. They might do this in order to ensure tight sequestration of the tumor suppressor protein. In the absence of p53, CaMK-II will therefore not form aggregates since its tumor suppressor substrate is not available to form a binding interaction (Figure 5A and B). Although my results show that CaMK-II aggregates do not completely co-localize with mitochondria (Figure 7), there could still be some form of interaction with the Bcl-2 family proteins that comprise and drive the mitochondrial p53 apoptotic pathway following prolonged G_0/G_1 cell arrest induced by the up regulation of $p27^{Kip1}$. A recent study has shown that CaMK-II clustering or self-association in neuronal cells form under ischemic conditions: low pH, low ATP levels, and the presence of Ca^{2+}/Calmodulin. When calmodulin binds to the regulatory region exposing the catalytic domains of CaMK-II, the autoinhibitory arm interacts with Thr^{286} on a CaMK-II monomer of an adjacent holoenzyme forming an inter-holoenzyme interaction (Vest et al., 2009). Another study using a mammalian kidney cell line showed that CaMK-II self-association is regulated by cellular pH and Thr^{286} autophosphorylation and has variable rates of dissociation depending on Ca^{2+} levels. Their data supports a novel mechanism for targeting CaMK-II to postsynaptic sites after neuronal activation forming a scaffold that recruits and localizes additional proteins to the postsynaptic density (Hudmon et al., 2005). It is possible that catalytically inactive CaMK-II could be acting in similar fashion by clustering in order to form a scaffold to recruit other proteins which aid in sequestering p53 in the cytosol.

The results that I obtained from the inhibition of CaMK-II using the chemical inhibitor KN-93 seems to also follow this model. However, because there was no evidence showing a significant difference between p53 knockdown and control HEK cells, the claim to support mitochondrial induced p53 apoptosis is less strong. In spite of this, the result is consistent with

previous work showing that KN-93 induces G_1 cell cycle arrest and could eventually lead to apoptosis following extended exposure to the drug (Tombes et al., 1995). Since KN-93 does not directly inhibit the catalytic activity of CaMK-II, pre-activated CaMK-II autophosphorylating independently of bound Ca^{2+} and CaM is unaffected by KN-93 inhibition (Schulman et al., 1992). KN-93 does not completely inactivate CaMK-II and therefore may not interact in the same way that dominant negative $K^{43}G$ or $K^{43}A$ CaMK-II mutants do with p53.

Another protein that could be involved with p53 and CaMK-II interaction is focal adhesion kinase (FAK). It has been shown that cell motility is inhibited upon FAK dephosphorylation by activated CaMK-II (Easley et al., 2008). Interestingly, FAK has also been implicated to bind to p53 in the cytoplasm (Cance and Golubovskaya, 2008). The overall reasons as to why FAK bind to p53 is unclear. It could be possible that when CaMK-II is inactivated, phosphorylated FAK stabilizes p53 thereby giving it the freedom to bind to CaMK-II in the cytosol.

In all, my thesis work has provided some initial insight to the functional understanding of the novel protein-protein binding interaction between CaMK-II and p53. I have also been able to assist in optimizing DNA and siRNA transfection protocols that will help expedite the process of making discoveries in future tissue culture studies in the lab. Additionally, I have developed not only more relatively efficient, but also reliable methods in obtaining, calculating, analyzing, and presenting numerical data acquired from fluorescent and phase contrast microscopic tissue culture images. The model that I have proposed from the data I have obtained in my project should be especially valuable in the planning of any future functional studies of CaMK-II and p53.

FIGURES

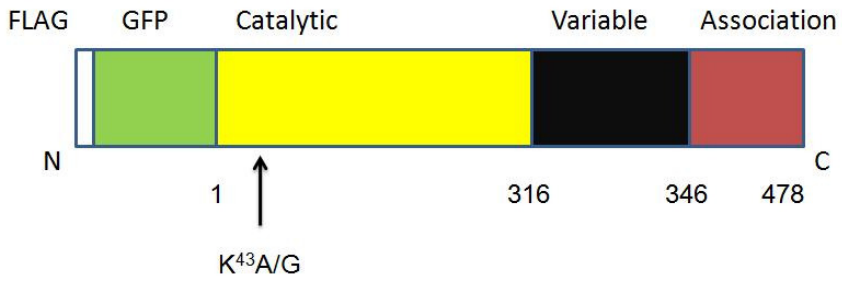

Figure 1. CaMK-II substrate trapping mutant structure. CaMK-II contains an amino-terminal catalytic domain, variable domain, and a carboxy-terminal association domain. The $K^{43}A/G$ point mutation was constructed in a previous project via PCR-mediated site-specific mutagenesis into the coding sequence of FLAG-GFP δ_e CaMK-II.

A.

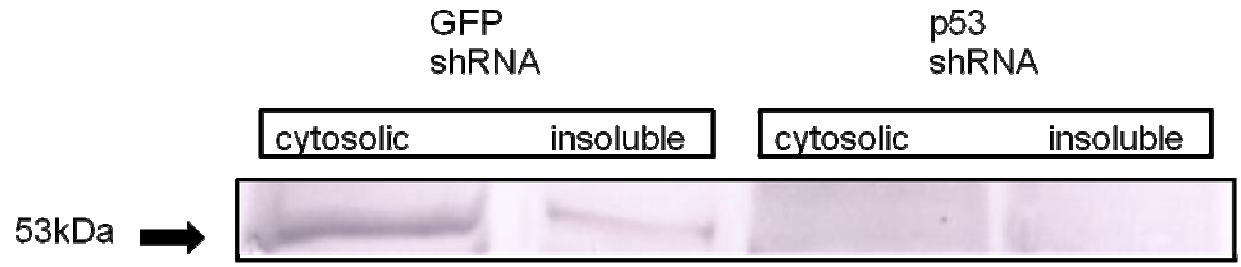

B.

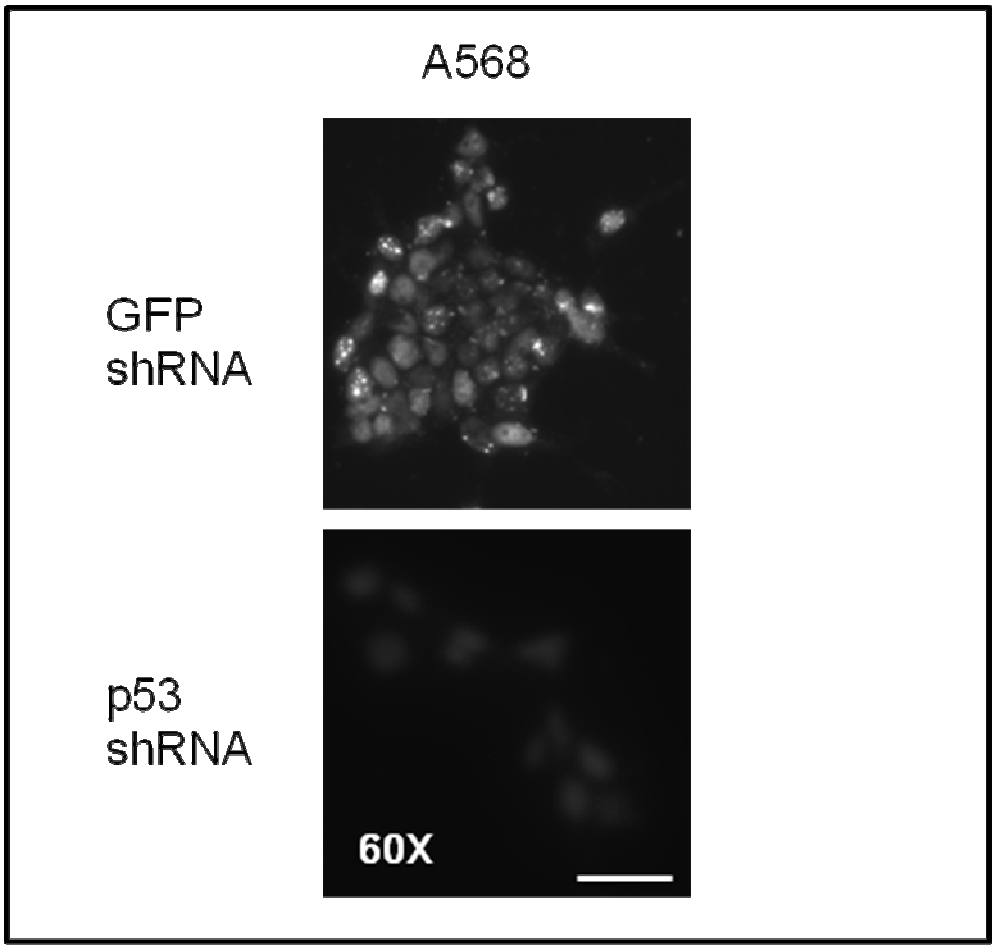

Figure 2. ***Stable p53 knockdown HEK cell line established. A.*** Immunoblot for p53 showing successful p53 knockdown in p53 shRNA lentivirally infected HEK cells in both the cytosolic and membrane fractions of the lysate. **B.** p53 immunostaining showing p53 significantly knocked down in p53 shRNA lentivirally infected HEK cells (A568 marking p53). Scale bar = 50 μm.

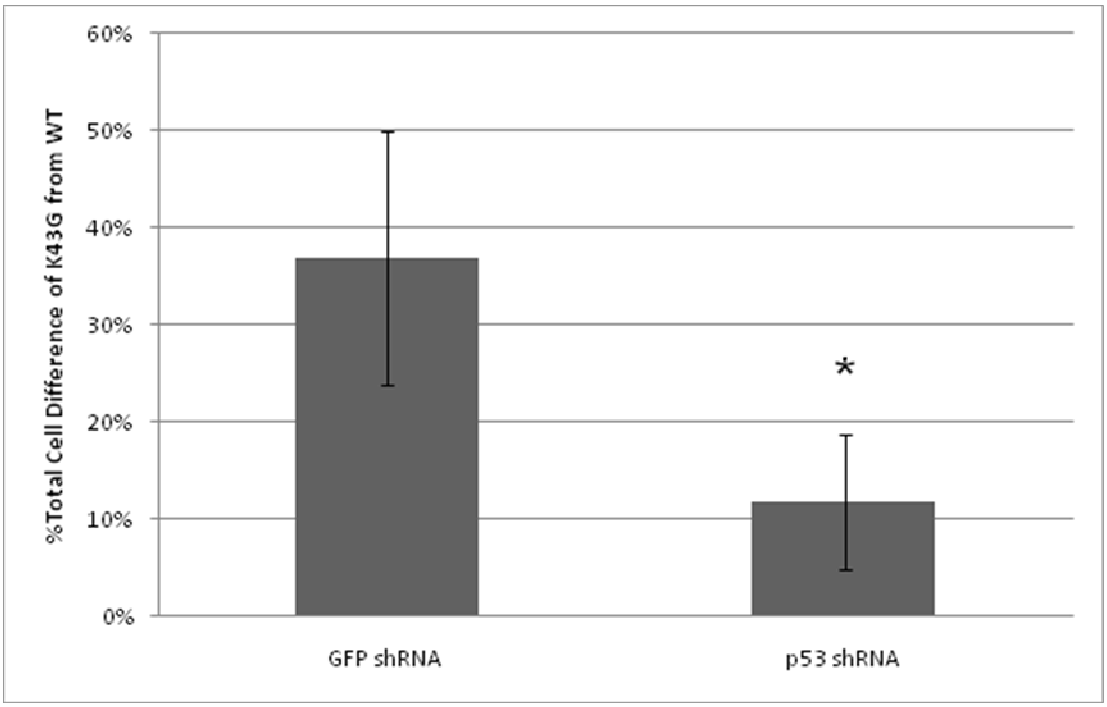

Figure 3. ***$K^{43}G$ CaMK-II inhibits cell growth in the presence of p53.*** DAPI staining was performed on HEK cells 48 hours after transfected with either $K^{43}G$ or WT CaMK-II. Total cells were counted and the percent difference between WT and $K^{43}G$ cells was calculated. p53 deficient cells were more growth inhibited compared to control cells. Graph represents the data from three separate experiments. Asterisk indicates p-value < 0.05.

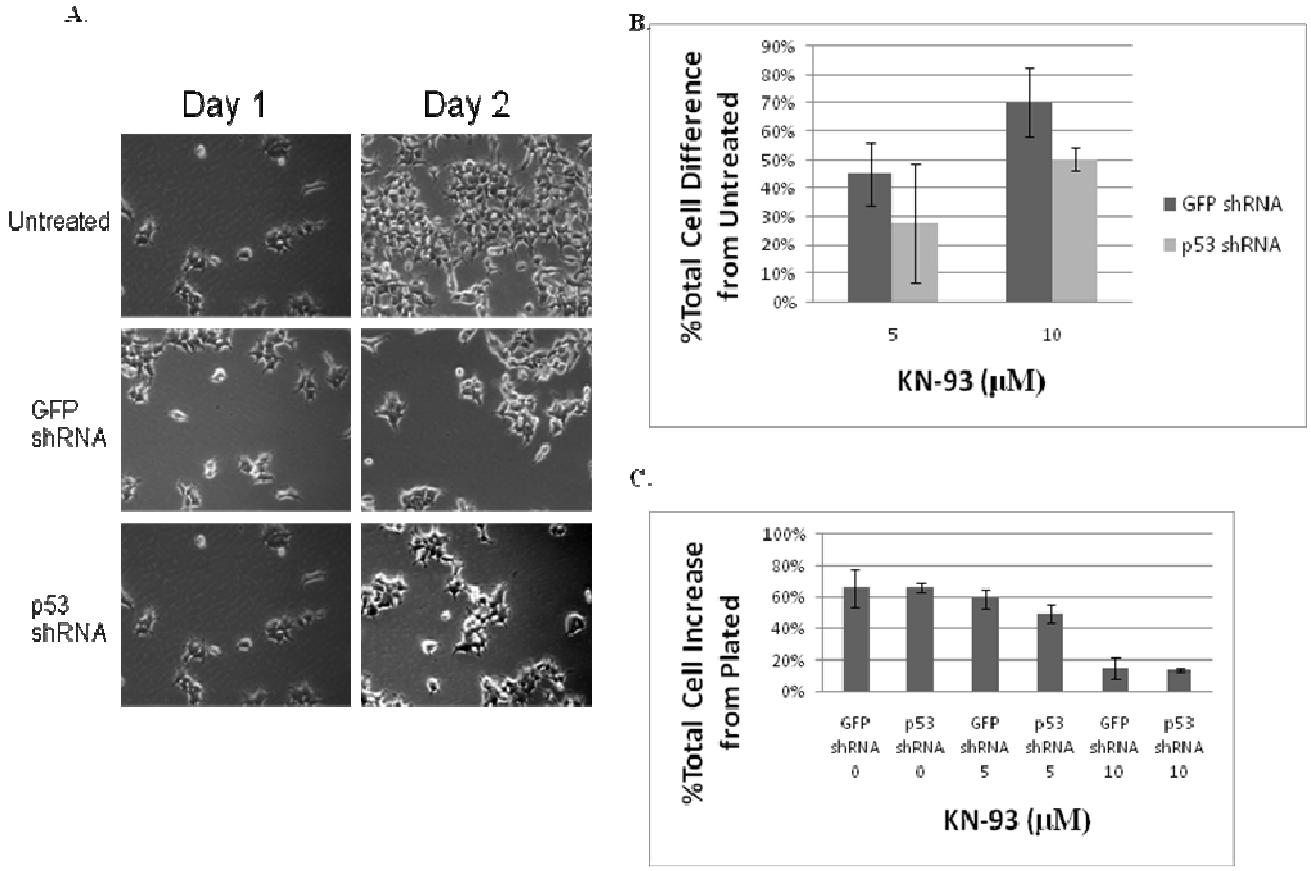

Figure 4. ***HEK cell growth is inhibited by KN-93 induced CaMK-II inhibition, but is not more sensitive in the absence of p53.*** **A.** Cells were counted when plated (Day 1) and 24 hours after KN-93 drug treatment (Day 2). Cell number did not increase in comparison to control when exposed to 10µM KN-93 for 24 hours (magnification = 20x). **B.** Cells were DAPI stained and counted 48 hours post KN-93 drug treatment. The percent difference of total cells was compared between KN-93 treated cells and untreated cells and showed no difference in p53 deficient cells. **C.** The percent increase of total cells from plated to 24 hours post treatment for each condition was calculated and analyzed. There was evidence of growth inhibition in cells treated with 10µM KN-93 for 24 hours. KN-93 was added in the amounts indicated (µM). Graphs represent the data from three separate experiments.

A.

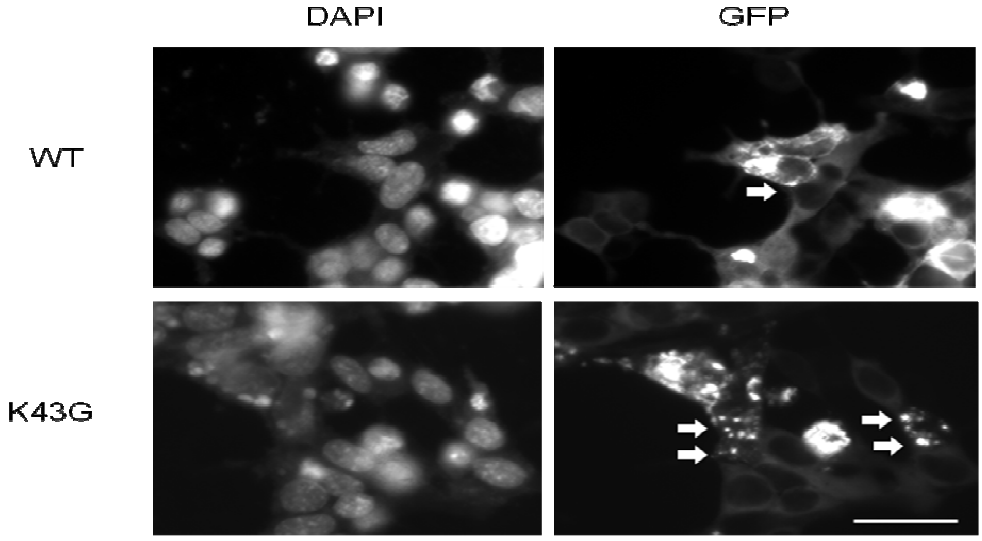

B.

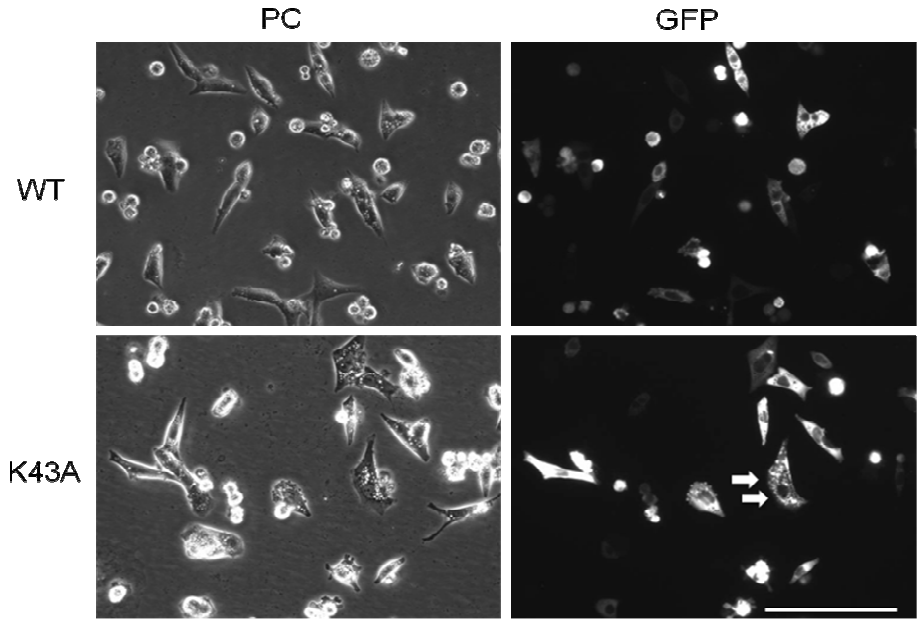

Figure 5. ***Dominant negative $K^{43}G/K^{43}A$ CaMK-II expression forms small aggregates in both HEK and mPCT cells.*** **A.** FLAG-GFP δ_e CaMK-II $K^{43}G$, WT. Images showing aggregates forming in both WT and $K^{43}G$ CaMK-II transfected HEK cells. More aggregates form in dominant negative $K^{43}G$ CaMK-II transfected cells (arrows; magnification = 60x). B. FLAG-GFP δ_e CaMK-II $K^{43}A$, WT. Images showing aggregates forming only in dominant negative $K^{43}A$ CaMK-II transfected mPCT cells (arrows; magnification = 20x).GFP is green fluorescent protein marking CaMK-II and DAPI marking cell nuclei. PC is phase contrast, DAPI is marking the nucleus, and GFP is green fluoresecent protein marking CaMK-II constructs. Top scale bar = 50 μm. Bottom scale bar = 100 μm.

A.

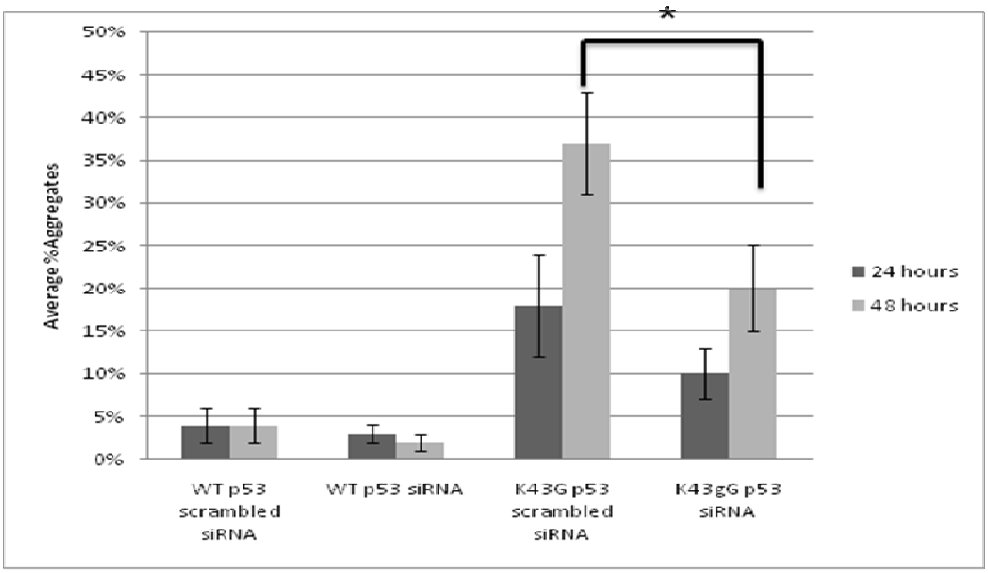

B.

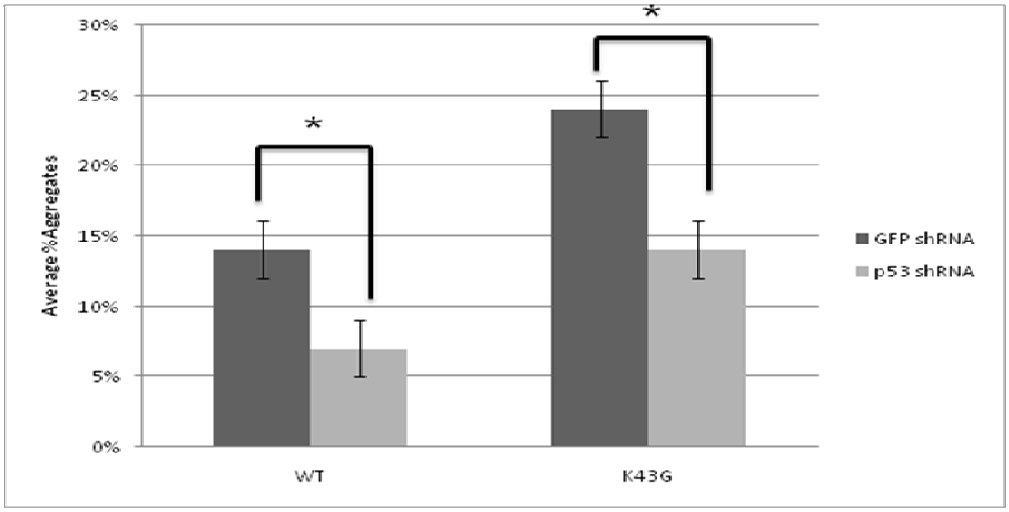

Figure 6. ***Less CaMK-II aggregates form in absence of p53.*** **A.** HEK siRNA transfection of either p53 siRNA or p53 scrambled siRNA co-transfected with WT or $K^{43}G$ CaMK-II fixed at 24 and 48 hours. Significantly more aggregation occurs in p53 deficient cells. **B.** Percentage of aggregates out of all transfected cells with WT or $K^{43}G$ CaMK-II fixed at 48 hours in the stable p53 knockdown HEK cells. CaMK-II aggregation increases in the absence of p53. Graphs represent the data from three separate experiments. Asterisks = p-value < 0.05.

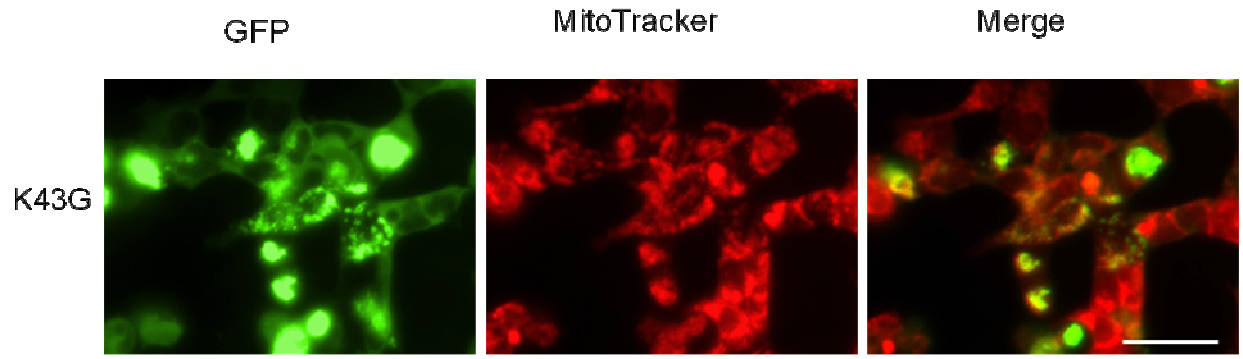

Figure 7. ***$K^{43}G$ CaMK-II aggregates might not be associated with the mitochondrial p53-pathway.*** Dominant negative $K^{43}G$ CaMK-II (GFP) and mitochondria stained (MitoTracker) do not co-localize in the cytosol of HEK cells (magnification = 60x; scale bar = 50 μm).

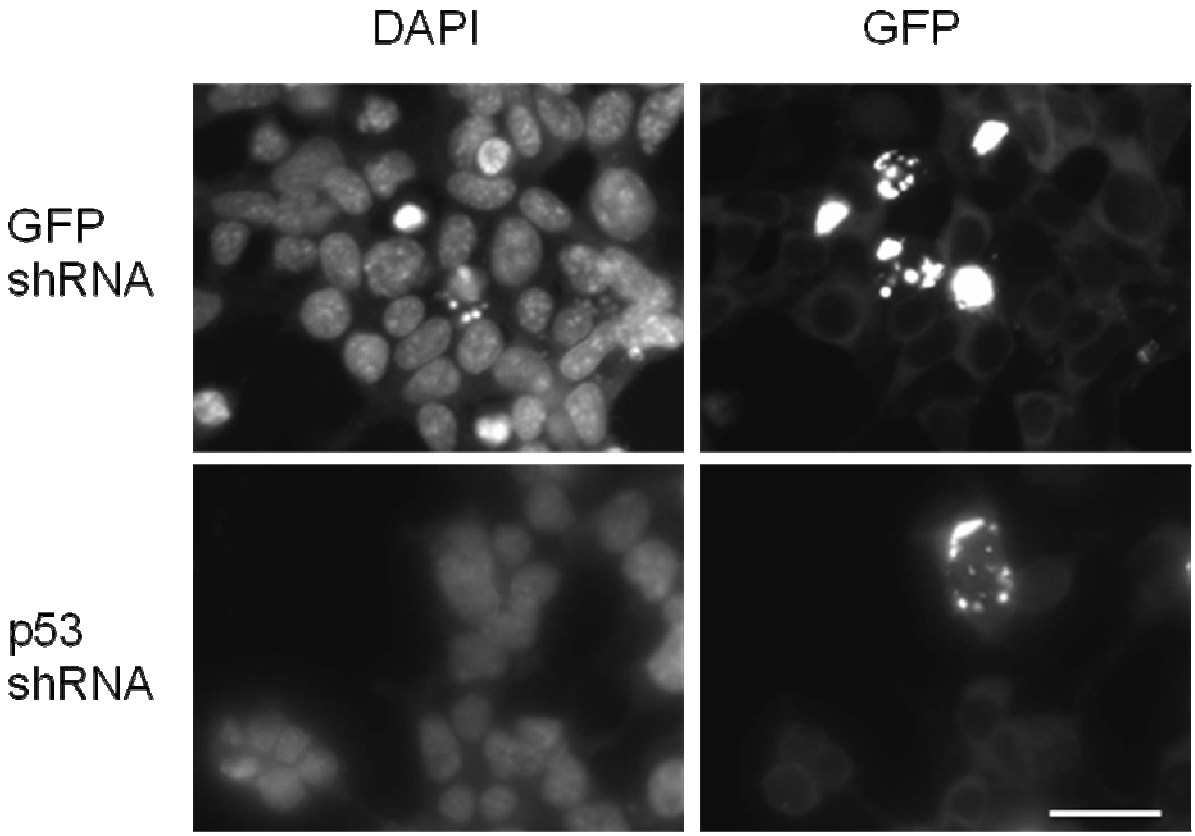

Figure 8. ***The interaction between CaMK-II and p53 does not involve the initiation of apoptosis.*** HEK cells transfected with $K^{43}G$ CaMK-II (GFP) does not show any evidence of chromatin fragmentation (DAPI). Scale bar = 50 μm.

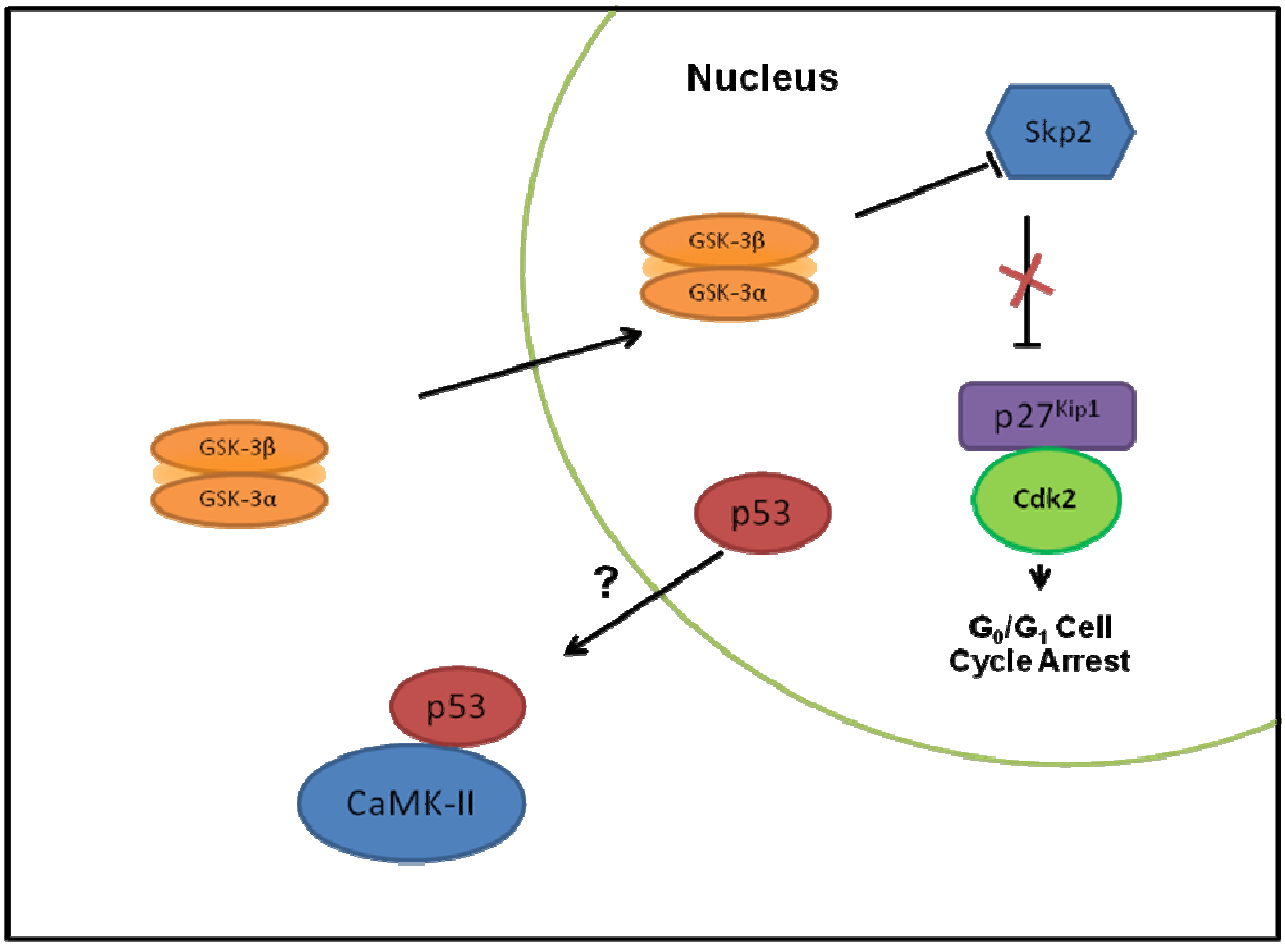

Figure 9. ***Model for the CaMK-II and p53 interaction.*** Catalytically inactive CaMK-II does not phosphorylate and thus cannot inactivate GSK-3α or GSK-3β. Activated GSK-3β enters the nucleus, down regulates SKP2 expression decreasing its inhibition on $p27^{Kip1}$. As a result, stabilized $p27^{Kip1}$ binds to Cdk2 causing G_0/G_1 cell cycle arrest. The mechanism describing how and why p53 is exported from the nucleus and is trapped by CaMK-II still remains unclear.

LITERATURE CITED

Abbas, T., and A. Dutta (2009). "p21 in cancer; intricate networks and multiple activities." Nature Reviews Cancer **9**(6): 400-14.

Amaral, J., J. Xavier, C. Steer, C. Rodrigues (2010). "The role of p53 in apoptosis". Discovery Medicine **9**(45): 145-52.

Blanchetot, C., M. Chanon, N. Dube, M. Halle and M. L. Tremblay (2005). "Substrate-trapping techniques in the identification of cellular PTP targets." Methods **35**(1): 44-53**.**

Basson, C T, D. R. Bachinsky, R. C. Lin, T. Levi, J.A. Elkins, J. Soults, D. Grayzel, E. Kroumpouzou, T.A. Traill, J. Lebanc-Straceski, B. Renault, R. Kucherlapati, J.G. Seidman, and C. E Seidman (1997). "Mutations in human tbx-5 cause limb and cardiac malformation in holt-oram syndrome." Nature Genetics **15**(1), 30-5.5.

Brooks CL, M. Li, and W. Gu (2007). "Mechanistic studies of mdm2-mediated ubiquitination in p53 regulation." Journal of Biological Chemisty **282**(31):22804-15, 2007.

Cance W. G., and V. M. Golubovskaya (2008). "Focal adhesion kinase versus p53: apoptosis or survival?" Science Signaling **1**(20): 120-122

Cohen, P, and S. Frame (2001). "The renaissance of GSK-3." Nature reviews Molecular Cell Biology **2**(10), 769-76.

Easley, C. A. iv., M. O. Faison, A. F. Horwitz and R. M. Tombes (2008). "CaMK-II promotes focal adhesion turnover and cell motility by inducing tyrosine dephosphorylation of FAK and paxillin." Cell Motility and the Cytoskeleton **65**(8): 662-74.

Faison, M. O., E. F. Perozzi, N. Caran, J. K. Stewart and R. M. Tombes (2002). "Axonal localization of delta Ca^{2+}/calmodulin, dependent protein kinase II in developing P19 neurons." International Journal of Developmental Neuroscience **20**(8): 585-92.

Fradet-Turcotte, A., C. Moody, L. A. Laimins, and J. Archambault (2010). "Nuclear export of human papillomavirus type 31 e1 is regulated by Cdk2 phosphorylation and required for viral genome maintenance." Journal of Virology **84**(22), 11747-60.

Francescatto, L., S. C. Rothschild, A. L. Myers, and R. M Tombes (2010). "The activation of membrane targeted CaMK-II in the zebrafish kupffer's vesicle is required for left-right asymmetry." Development **137**: 2753-62.

Hanks, S.K., A. M. Quinn and T. Hunter (1988). "The protein kinase family: conserved features and deduced phylogeny of the catalytic domains." Science **241**(4861): 42-52.

Hudmon, A.and H. Schulman (2002). "Neuronal Ca^{2+}/calmodulin-dependent protein kinase II: the role of structure and autoregulation intercellular function". Annual Review of Biochemistry **71**: 473-510.

Hudmon, A., Lebel E., Roy H., Sik A., Schulman H., Waxham M. N. and P. De Konick (2005). "A mechanism for Ca^{2+}/Calmodulin dependent protein kinase II clustering at synaptic and nonsynaptic sites based on self-association." The Journal of Neuroscience **25**(30):6971-83.

Klein P.S., and D.A. Melton (1996). "A molecular mechanism for the effect of lithium on development". Proceedings of the National Academy of Sciences **93**(16):8455-9

Kolb, S.J., A. Hudmon, T.R. Ginsberg, and M.N. Waxham (1998). "Identification of domains essential for the assembly of calcium/calmodulin-dependent protein kinase II holoenzymes." Journal of Biological Chemistry. **273**:31555-64.

Kuttenkeuler D., and M. Boutros. (2004). "Genome-wide RNAi as a route to gene function in Drosophila." Briefings in Functional Genomics. **3**(2) :168-176

Lane, D P (1992). "Cancer. p53, guardian of the genome." Nature **358**(6381):15-6.

Lantsman, K., and R.M. Tombes (2005). "CaMK-II oligomerization potential determined using CFP/YFP FRET." Biochimica et Biophysica Acta. **1746**:45-54.

Lohrum M. A. E., D.B. Woods, R. L. Ludwig, E. Balint, and K. H. Vousden (2001). "C-terminal ubiquitination of p53 contributes to nuclear export." Molecular and Cellular Biology. **21**(24):8521-8532.

Li M, J. Luo, C. L. Brooks, and W. Gu (2011). "Acetylation of p53 inhibits its ubiquitination by mdm2." Journal of Biological Chemistry **277**(52):50607-11, 2002.

Li, N, C. Wang, Y. Wu, X. Liu, and X. Cao (2009). "Ca(2+)/calmodulin-dependent protein kinase ii promotes cell cycle progression by directly activating mek1 and subsequently modulating p27 phosphorylation." Journal of Biological Chemistry, **284**(5), 3021-7.

Li W., H. Li, P. N. Sanders, P. J. Mohler, J. Backs, E. N. Olson, M. E. Anderson and I. M. Grumbach (2011). "The multifunctional Ca^{2+}/Calmodulin-dependent kinase II δ (CaMK-IIδ) controls neointima formation after carotid ligation and vascular smooth muscle cell proliferation through cell cycle regulation by p21." Journal of Biological Chemistry **286**: 7990-7999.

Ma S.,Y. Yang, C. Wang, N. Hui, L. Gu, H. Zhong, Z. Cai, Q. Wang, Q. Zhang,N. Li, and X. Cao (2009). "Endogenous Human CaMK-II inhibitory protein suppresses tumor growth by inducing cell cycle arrest and apoptosis through down-regulation of the phosphatidylinositide 3-kinase/Akt/HDM2 pathway." Journal of Biological Chemistry. **284**: 24773-24782

Morris, T.A., R.J. DeLorenzo, and R.M. Tombes (1998). "CaMK-II inhibition reduces cyclin D1 levels and enhances the association of $p27^{Kip1}$ with Cdk2 to cause G_1 arrest in NIH 3T3 cells." Experimental Cell Research. **240**:218-27.

Muller, P. A. J., Vousden, K. H., and J. C. Norman (2011). "p53 and its mutants in tumor cell migration and invasion." The Journal of Cell Biology **192**(2):209-18.

Osterhoff, M., M. Mohlig, M. Schwanstecher, J. Seufert, J. Ortmann, H. Schatz

and A. F. Pfeiffer (2003). "Ca^{2+}/calmodulin-depending protein kinase II delta2 regulates gene expression of insulin in INS-1 rat insulinoma cells." Cell Calcium **33**(3): 175-84.

Pattanayak D., S. Agarwal, S. Sumathi, S. K. Chakrabarti, P. S. Naik, and S. M. Khurana (2005). "Small but mighty RNA-mediated interference in plants." Indian Journal of Experimental Biology **48**(3):248-257.

Price, B D, L. Hughes Davies, and S. J. Park (1995). "Cdk2 kinase phosphorylates serine^{315} of human p53 in vitro." Oncogene **11**(1), 73-80.

Resnitzky, D., M. Gossen, H. Bujard and S. I. Reed (1994). "Acceleration of the G_1/S phase transition by expression of cyclins D1 and E with an inducible system." Molecular and Cellular Biology **14**(3): 1669-79.

Rothschild, S.C., C. A. iv. Easley, L. Francescatto, J.A. Lister, D. M. Garrity, and R. M. Tombes (2009). "Tbx-5-mediated expression of Ca2+/calmodulin-dependent protein kinase II is necessary for zebrafish cardiac and pectoral fin morphogenesis." Developmental Biology. **330**(1):175-184.

Schulman, H, P. I. Hanson, and T. Meyer (1992). "Decoding calcium signals by multifunctional cam kinase." Cell Calcium **13**(6-7), 401-11.

Seward, M. E., C. A. iv. Easley, J. J. McLeod, A. L. Myers and R. M. Tombes (2008). "Flightless-I, a gelsolin family member and transcriptional regulator preferentially binds directly to activated cytosolic CaMK-II." FEBS Letters **582**(17): 2489-95.

Song, B., B. Lai, Z. Zheng, Y. Zhang, J. Luo, C. Wang, Y. Chen, J.R. Woodgett, and M. Li (2010). "Inhibitory phosphorylation of GSK-3 by CaMK-II couples depolarization to neuronal survival." Journal of Biological Chemistry **285**(52), 41122-34.

Tombes, R.M., M.O. Faison and J. M. Turbeville (2003). "Organization and evolution of multifunctional Ca^{2+}/CaM-dependent protein kinase genes." Gene **322**: 17-31.

Tombes, R.M., Westin, E., Grant, S., and Krystal, G. (1995). G_1 cell cycle arrest and apoptosis are induced in NIH 3T3 cells by KN-93, an inhibitor of CaMK-II. Cell Growth and Differ. **6**:1063-1070.

Vest, R. S., O'Leary H., and K. U. Bayer (2009). "Differential regulation by ATP versus ADP further links CaMK-II aggregation to ischemic conditions." FEBS letters **583**(22) :3577-81.

Wang, C. N. Li, X. Liu, Y. Zheng and X. Cao (2008). "A novel endogenous human CaMK-II inhibitory protein suppresses tumor growth by inducing cell cycle arrest via p27 stabilization." Journal of Biological Chemistry **283**(17): 11565-74.

Wang, Q, Y. Zhou, X. Wang, and B. M. Evers (2008). "$p27^{Kip1}$ nuclear localization and cyclin-dependent kinase inhibitory activity are regulated by glycogen synthase kinase-3 in human colon cancer cells." Cell Death and Differentiation **15**(5), 908-19.

Yoshimura, Y., T. Shinkawa, M. Taoka, K. Kobayashi, T. Isobe and T. Yamauchi (2002). "Identification of protein substrates of Ca^{2+}/calmodulin-dependent protein kinase II in the postsynaptic density by protein sequencing and mass spectrometry." Biochemical and Biophysical Research Communications **290**(3): 948-54.

VITA

Raymond Eugene Lai was born in Fairfax, Virginia on October 27th, 1986 and currently resides in Richmond, VA. He received his Bachelor's of Science degree in biology from the College of William and Mary May, 2009 in Williamsburg, Virginia.